Mine Water Environ (2016) 35:508–524
DOI 10.1007/s10230-015-0370-4

TECHNICAL ARTICLE

Tailings Weathering and Arsenic Mobility at the Abandoned Zgounder Silver Mine, Morocco

M. El Adnani[1,4] · B. Plante[2] · M. Benzaazoua[2,4] · R. Hakkou[3,4] · H. Bouzahzah[2]

Received: 13 January 2015 / Accepted: 4 October 2015 / Published online: 26 October 2015

Abstract The abandoned Zgounder Mine (Morocco) was exploited for Ag from 1982 to 1990 and generated nearly 490,000 t of mill tailings before it was closed without being reclaimed. The tailings contain low concentrations of sulfide (mainly as pyrite, sphalerite, and galena) and carbonates (mainly dolomite). Silicates (muscovite, albite, chlorite, labradorite, actinolite, and orthoclase) occur in high concentrations. The most abundant trace elements are As, Ti, Fe, Mn, Zn, and Pb. We studied the geochemical behavior of the mine wastes to identify the main factors controlling drainage water chemistry. Particular emphasis was put on sorption phenomena to explain the low As concentrations in the leachates despite significant As levels in the tailings. Weathering cell tests carried out on various tailings produced two types of contaminated drainage: acidic and neutral. The kinetic test leachates contained high concentrations of some contaminants, including As (0.8 mg L^{-1}), Co (11 mg L^{-1}), Cu (34 mg L^{-1}), Fe (70 mg L^{-1}), Mn (126 mg L^{-1}), and Zn (314 mg L^{-1}). Acidity and contaminants in the leachates were controlled by dissolution of soluble salts and Fe hydrolysis rather than sulfide oxidation. Batch sorption tests quantified the significance of As sorption, and sequential extraction showed that most of the As sorption was associated with the reducible fractions (Fe and Mn oxides and oxyhydroxides).

Keywords Acid mine drainage · Contaminated neutral drainage · Sorption · Weathering cells · Geochemical behavior

Introduction

Mining of metallic ore deposits can expose sulfide minerals to atmospheric weathering. Consequently, the sulfide minerals can oxidize and produce acidic water laden with sulfate, metals, and metalloids, known as acid mine drainage (AMD) (Akcil and Koldas 2006; Harris et al. 2003). When sufficient neutralization capacity is available within the mine wastes, leachate pH remains near neutral, but the water can still contain metals that exceed regulatory water pollution standards; in this case, the effluent corresponds to contaminated neutral drainage (CND) (Beauchemin and Kwong 2006; Plante et al. 2010). Both AMD and CND can threaten surrounding ecosystems, especially biodiversity (Lei et al. 2010; Niyogi et al. 2002). Mine drainage is controlled by natural factors such as the geology, hydrology, and geochemistry of the mine area (Cheng et al. 2009; Fukushi et al. 2003). Geochemical phenomena, such as oxidation, acid neutralization, precipitation, sorption, hydrolysis, and solubilization, which occur at different reaction rates, often affect contaminant mobility (Fukushi et al. 2003; Haffert et al. 2010; Harris et al. 2003; Mahoney et al. 2005).

Arsenic (As) is known for its association with sulfide minerals, mainly in gold-silver ore deposits (Haffert et al.

Electronic supplementary material The online version of this article (doi:10.1007/s10230-015-0370-4) contains supplementary material, which is available to authorized users.

✉ M. El Adnani
eladnani@gmail.com; eladnani@enim.ac.ma

1 Ecole Nationale Supérieure des Mines de Rabat, Ave Hadj Ahmed Cherkaoui, BP 753, Agdal, Rabat, Morocco

2 Univ du Québec en Abitibi Témiscamingue, 445 Boul de l'Université, Rouyn-Noranda, QC J9X 5E4, Canada

3 LCME, Faculté des Sciences et Techniques, Univ Cadi Ayyad, BP 549, 40000 Marrakech, Morocco

4 IDRC Research Chair in Management and Stabilization of Mining and Industrial Wastes, Marrakech, Morocco

2010; Kim et al. 2012). The release of As from contaminated sites is controlled by dissolution/precipitation processes (Fukushi et al. 2003; Haffert et al. 2010; Mahoney et al. 2005) and by sorption phenomena. Sorption of As is a complex process based on interrelations between the properties of the solid surface, temperature, pH, and the concentration and speciation of As and competing ions (Asta et al. 2009; Cheng et al. 2009; Lizama et al. 2011; Mamindy-Pajany et al. 2011). Aqueous arsenite species [As(III)] predominate in reducing environments, whereas arsenate species [As(V)] are more abundant under oxidizing conditions, and are considered to be both less toxic and mobile (Bagherifam et al. 2014; Lizama et al. 2011). The major species in mine water are H_3AsO_4 and $H_2AsO_4^-$ for As(V) and H_3AsO_3 for As(III) (Smedley and Kinniburgh 2002). These As oxyanions (either arsenite or arsenate) are prone to sorption onto positively charged surfaces (Appelo and Postma 2005). Various mineral surfaces are able to sorb arsenic, including Fe, Al, and Mn oxyhydroxides, clays, carbonate, and organic matter (Cheng et al. 2009). Fe oxyhydroxides are considered to be some of the best As sorbents (Carrillo and Drever 1998; Foli et al. 2013; Giménez et al. 2007; Mamindy-Pajany et al. 2011), and their high affinity for As is useful for As removal from water (Carrillo and Drever 1998), mine tailings (Kim et al. 2012), soils (Drahota et al. 2012), and sediment (Mamindy-Pajany et al. 2011). These properties also contribute to As attenuation in mine water. However As can also be desorbed from sorption sites by changing geochemical and hydrological (pH, competition, etc.) conditions (Asta et al. 2009; Foli et al. 2013; Mahoney et al. 2005; Mamindy-Pajany et al. 2011).

About 200 mines in Morocco were abandoned without considering structural stability and potential environmental risks. The Zgounder deposit is one of the oldest and most famous silver deposits in Morocco. It is located in the western part of the central Anti-Atlas Mountain Range, 150 km south of Marrakech, at an altitude between 2000 and 2150 m, on the flanks of the Siroua mountains (Fig. 1). The local relief is hilly with a valley that contains the Zgounder River. The region has a continental climate; temperatures range from −5 °C in January to 20 °C in July. Average annual rainfall is around 419 mm and is concentrated in the months of December–February. The geology consists of a volcanic/sedimentary formation, attributed to the Precambrian, which overlies an andesitic basement that outcrops in the north of the district. The silver mineralization (mainly as acanthite Ag_2S, polybasite $Ag_{16}Sb_2S_{11}$, and pearceite $Ag_{16}As_2S_{11}$) occurs as intermittent lenses of varied sizes in the host rock. Within the ore body, Ag mineralization occurs in mm-sized veins that are mainly pyritic, as disseminated fine particles in the host rock, and in veinlets with quartz/sulfides that occur in centimeter-sized cracks. Native silver (Ag–Hg amalgam) is the most commonly found silver mineral, representing 65–90 % of the silver ore (Macroux and Wadjinny 2005).

The deposit was intermittently mined between the thirteenth and nineteenth centuries, and later by the SOMIL Co., which was a part of ONHYM (National Office of Hydrocarbons and Mines, Morocco), between 1982 and 1990. During this period, about 500,000 t of ore, containing approximately 300 g/t of Ag, were mined. Ore processing was done by crushing and milling followed by extraction using cyanide. More than 490,000 t of tailings were deposited in the north tailings pond (≈38 ha), from 1982 to 1988, and in the south tailings pond (≈18 ha), from 1988 to 1990 (Fig. 2a–c). The bottoms of the two tailings ponds are unlined and have not prevented infiltration of surface mine drainage waters. Both tailings ponds show yellow and reddish seepage resulting from rainwater infiltration. The seepages flow along a tributary and join the Zgounder River. The site was closed in 1990 and left without remediation. The north tailings pond dam was built using tailings and gabion structures that successively collapsed, leaving tailings distributed along the slope to the river (Fig. 2d). Waste rock and other tailings were also stored on the flanks of the hills, close to the mine gallery entrances, and in the old river bed (Fig. 2d).

We studied the geochemical behavior of the site's mine wastes to identify the main factors controlling drainage water chemistry, in particular metal and metalloid dissolution, from the mine tailings. Initially, the mine wastes were characterized to determine their mineralogical and chemical composition, and secondary mineralogy. In a second step, the samples were characterized for their principal physical features and their acid generation potential using static tests. Third, the geochemical behavior of the tailings was evaluated using weathering cells. Finally, As sorption was studied using sorption and extraction tests to better understand the phenomena that control As concentrations in the site's mine drainage.

Materials and Methods

Tailings Sampling and Analysis

In June 2013, two 60 cm deep trenches (T1 and T2) were excavated in the north tailings pond, and one 60 cm deep trench was excavated in the south tailings pond (T3) (Fig. S1) (note: figures denoted in this fashion are supplemental and accompany the on-line version of the manuscript; these figures can easily be downloaded for free.) No color change was observed along the depth profile of trenches T1 and T3. Hence, samples were taken at the surface (ZG1 and ZG6 respectively) and the potentially

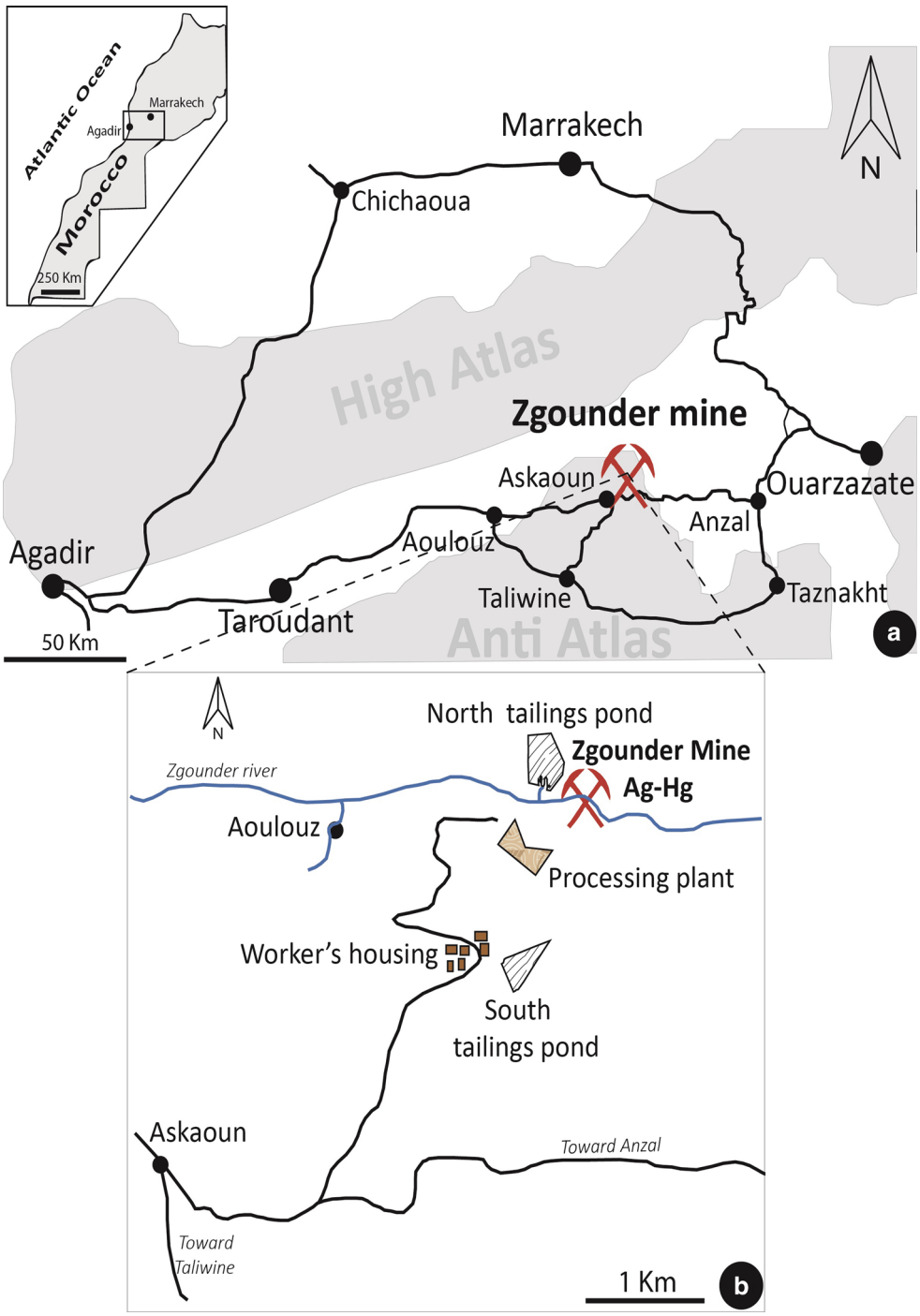

Fig. 1 Location map of the Zgounder Mine: regional mine situation (**a**), zoom showing location of tailings ponds and the watershed (**b**)

fresh or 'unaltered' tailings at 60 cm depth (ZG2 and ZG7 respectively) (Fig. S1a, c). At trench T2 (north tailings pond), three horizons were identified and sampled (Fig. S1b). ZG3 was taken at the surface (0 cm), while ZG4, which had a yellowish coloration, was sampled from 15 to 20 cm deep, and ZG5 (blackish-gray in color) was taken at a depth of 60 cm.

Precipitates and secondary efflorescent salts, recognizable by their distinct colors (white, turquoise, red, and yellow), were more abundant in the north tailings pond. Whitish phases were the most abundant in both tailings ponds. Different secondary minerals covering the tailings were sampled (M1–M4). A sample of a reddish precipitate from the north tailings pond seepage was also collected (M5). All samples were carefully collected, transported to the laboratory, and stored in double-sealed plastic bags after air evacuation. The fine tailings were dried in an oven at 40 °C.

Fig. 2 Photographs showing an overview of the mine site and processing plant (**a**), tailings ponds (**b** North, and **c** South), tailings dispersed after collapse of north tailings pond dam, and waste rock disposed in the river bed (**d**)

Particle size distribution was determined using a Malvern Mastersizer laser particle size analyzer (Merkus 2009). Specific gravity (Gs) was measured using a micromeritics helium pycnometer. The specific surface (Ss) area was determined with a micromeritics Ss analyzer using the BET method (Brunauer et al. 1938). The chemical compositions of the tailings were determined using acid digestion (HNO_3–Br_2–HF–HCl) (Potts 1987), followed by ICP-AES analysis for over 20 elements, to a 0.001 wt% precision. Some elements (As, Be, Bi, Sb, Se, Te, and Si) were partially evaporated during the digestion procedure. They were analyzed separately after adaptation of the digestion procedure, but silicon was not determined for the present study. Sulfide sulfur was determined by subtraction of the sulfate sulfur (determined by a 40 % HCl extraction with 0.001 wt% precision; Sobek et al. 1978) from the total sulfur (ICP AES analysis). Mineralogical characterization was performed only for the "unaltered" samples (ZG2, ZG5, and ZG7), initially with a Bruker A.X.S. D8 X-ray diffraction (XRD) instrument, with a detection limit and precision of $\approx$0.1–0.5 wt%. Mineralogical quantification was realized with Rietveld (1993) fitting of the XRD data using the TOPAS software. Mineralogical analyses were completed on polished sections of the tailings samples using a Zeiss Axio optical polarizing microscope and a Hitachi S-3500N scanning electron microscope (SEM) coupled with an Oxford Instruments energy dispersive X-ray spectroscopy (EDS) probe.

Static tests were conducted in order to assess the acid generation potential of samples ZG2, ZG5, and ZG7. The neutralization potential (NP) was determined by the standard carbonate NP method, which is based on the measurement of the total inorganic carbon with an induction furnace and its conversion into kg $CaCO_3$/t equivalents (Lawrence et al. 1989). Inorganic carbon can be used in this study, as the tailings do not contain Fe and/or Mn carbonates (such as ankerite and siderite), which can neutralize initially and produce acidity after Fe/Mn oxidation and hydrolysis (Skousen et al. 1997). This method is simple and widely used in the industry (Frostad et al. 2003). The acid generation potential (AP), also expressed in kg $CaCO_3$/t, was calculated by using the sulfide sulfur fraction, obtained by subtracting the sulfate sulfur from the total sulfur assay (Lawrence and Wang 1996). The net neutralization potential (NNP) was calculated by subtracting the AP value from the NP value. NNP values less than -20 kg $CaCO_3$/t indicate an acid-producing material, whereas materials with NNP >20 kg $CaCO_3$/t are considered to be acid consuming. Hence, some uncertainty for this technique exists between $-20 < \text{NNP} < 20$ kg $CaCO_3$/t (Miller et al. 1991; SRK 1989). Another tool used to evaluate the AMD production potential from static tests is the NP–AP ratio. Typically, the material is considered

non-acid generating if NP/AP >2.5, uncertain if 2.5 > NP/AP > 1, and acid generating if NP/AP <1 (Adam et al. 1997).

Leaching Tests

Leaching tests are performed to assess leaching of potentially toxic elements from these materials under specific conditions. In this study, the test was performed according to the CTEU-9 method (Expertise Center in Environmental Analysis of Quebec 2012) for determining the concentration of inorganic species likely to be leached on contact with neutral pH water. A modified solid/liquid (S/L) ratio of 1:25 (the original is 1:4) was used in order to get the same ratio as the sorption tests. Therefore, 1 g of solid was leached with 25 mL of water and shaken for 7 days at room temperature. Additional testing durations (2, 6, 24, and 72 h) were used to monitor behavior during the first hours of contact with water. At each water sampling, leachates were filtered using a 0.45 µm nylon filter and acidified with 2 % HNO_3. The resulting solutions were analyzed by ICP-AES.

Weathering Cell Tests

The tailings geochemical behavior study was carried out in weathering cells, which are small-scale kinetic tests that require a small amount of material (Cruz et al. 2001; Hakkou et al. 2008; Villeneuve et al. 2004). Approximately 66.7 g (dry weight) of tailings ZG2, ZG5, and ZG7 were placed in a 100 mm diameter Buchner funnel equipped with a glass fiber filter. A 7-day cycle consisted of two flushing days (typically Mondays and Thursdays) alternating with 2 and 3 days of exposure to ambient air, respectively. The flushes consisted of adding 50 mL of deionized water to the top of the Buchner funnel. The leachate was recovered by applying a slight suction on a filtering flask after 3 h of contact with the tailings. The ZG2 and ZG7 weathering cell tests were dismantled earlier than the ZG5 test due to perforation of their filters.

The leachates obtained during the weathering cell tests were filtered using a 0.45 µm pore size nylon filter and analyzed for several geochemical parameters in order to understand the sulfide reactivity, oxidation kinetics, metal solubility, and overall leaching behavior of the tested materials. Filtered leachates were acidified with 2 % HNO_3 to avoid metal precipitation and analyzed with ICP-AES to determine metal and sulfate concentrations (in mg L^{-1}). For each kinetic test cycle, the pH, Eh, electrical conductivity (EC), metal concentrations, acidity, and alkalinity were analyzed for each leachate sample. Alkalinity and acidity (expressed in mg $CaCO_3$/L) were measured by acid–base titration to pH endpoints of 8.3 and, 4.5, respectively. Sample pH, redox potential, and EC were measured with an Accumet excel XL60 dual channel pH/ion/conductivity/DO meter. Redox potential results were corrected to a standard hydrogen electrode (SHE). These data were compiled as instantaneous and cumulative loads based on the volume and composition of the leachates, and normalized to the solid samples mass.

Batch Sorption Tests

The As sorption capacity of the tailings was investigated using static and kinetic batch sorption tests on samples ZG2, ZG5, and ZG7. Because conditions are oxidizing in weathering tests, As in the leachates is most likely in the arsenate form (Mamindy-Pajany et al. 2011). Therefore, an arsenate stock solution, prepared from a sodium arsenate salt ($AsHNa_2O_4{\cdot}7H_2O$), was used for all sorption tests. An initial L/S ratio of 25:1 mL g^{-1} was chosen for all of the batch sorption tests, which allowed sufficient solution for sampling during the experiments. Ionic strength was adjusted to 0.05 M with $NaNO_3$. The ionic strength adjustments limit the effect of a change in ion concentrations on the sorption properties; with a high ionic strength, the composition of the background solution can be considered constant (Limousin et al. 2007; Plante et al. 2010). Previous studies (Asta et al. 2009; Mamindy-Pajany et al. 2009) have shown that As(V) sorption is independent of the solution ionic strength. However, those studies were performed on pure minerals (hematite, goethite, and jarosite) and with As concentrations and sample masses that were much lower than those in this study. The experimental conditions conducted in this work were chosen after preliminary sorption tests designed from common batch sorption tests found in the literature (Carrillo and Drever 1998; Giménez et al. 2007; Mamindy-Pajany et al. 2011).

Kinetic sorption tests were first performed to determine the time necessary to reach equilibrium. Then, the static batch tests were conducted, considering the equilibrium time previously determined. The kinetic sorption tests were carried out with 10 mg L^{-1} As for all samples, with reaction times of 2, 6, 24, and 72 h. The static tests were conducted to study the As sorption as a function of pH (pH 4, 5, 6, and 7), at a constant As concentration (10 mg L^{-1}) and a constant ionic strength (0.05 M). The initial pH was chosen to cover the pH range observed in the preliminary kinetic tests and in the field. The pH was adjusted using 0.02 M H_2SO_4 and NaOH solutions. Batch tests were also conducted as a function of initial As concentration (0.1, 1, 10, and 50 mg L^{-1}) at constant pH and ionic strength (0.05 M). The concentrations 0.1 and 1 mg L^{-1} are close to those obtained in the weathering cells. The 10 and 50 mg L^{-1} concentrations were considered respectively as high and "extreme" concentrations to evaluate the

"maximum" As sorption capacity. After a predetermined contact time, the aqueous samples were decanted, filtered through 0.45 μm nylon filters, acidified with 2 % HNO_3, and analyzed by ICP-AES.

Sequential Extraction Tests

Selective sequential chemical extractions are often used to determine the metal distribution with different sorptive phases and metals mobilization in soils and mine wastes (Dold 2003; García-Sánchez et al. 2010; Pöykiö et al. 2002; Tessier et al. 1978). The general principle is to leach the sample with increasingly strong reagents, chosen for their reaction selectivity. At each stage, the metals and metalloids bound to a particular geochemical fraction are released into the solution by ion exchange or dissolution. Sequential chemical extractions are considered as semi-quantitative, evaluating the nature and quantity of sorption processes in soils and mine wastes (Plante et al. 2010).

The sequential extraction method used in this study was adapted from Neculita et al. (2008) and can be described as follows: (1) the soluble and easily exchangeable phases were extracted using 0.5 M $MgCl_2$ (L/S ratio: 24/1) at pH 7 for 1 h at room temperature; (2) the acid-soluble phases were extracted with 1 M sodium acetate (L/S ratio: 24/1) at pH 5 for 5 h at room temperature; and (3) the reducible phases were extracted with NH_2OH–HCl 0.04 M in 25 % acetic acid (L/S ratio: 36/1) for 6 h at room temperature. Sequential extractions were conducted successively on initial and post-testing samples (ZG2, ZG5, and ZG7). The extractions were performed in duplicate on 1 g aliquots under ambient air on a rotary shaker at 250 RPM to minimize any diffusion-related bias. The samples were rinsed twice with deionized water after a chemical extraction step to minimize possible carryover between extraction steps; these water extracts were combined with the corresponding chemical extraction for metal analysis.

Results

Physical, Chemical, and Mineralogical Properties

The physical, chemical, and mineralogical characteristics of the samples are summarized in Table 1. The relative densities (G_s) show similar values for the different tailings samples. The grain size distributions show that the south tailings pond samples were coarser than those of the north tailings pond. This might be related to ore processing changes that occurred during the mine life. In addition, in the two trenches of the north tailings pond, the surface samples had larger particle sizes (D_{80}: 83–95 μm) than the bottom samples (D_{80}: 35.2–40.5 μm). However, for the south pond trench samples, the D_{80} were higher, but the samples at the bottom were coarser than the ones from the surface. The same trends were observed for D_{10} and D_{90}.

Particle size differences explain the S_s areas observed for the samples (Table 1). The S_s values at the bottom of the north tailings pond (ZG2 and ZG5) were higher than those at the bottom of the south tailings pond (ZG7). These high S_s reflect the presence of phyllosilicate minerals that are well known for their high S_s areas.

The chemical analyses of the Zgounder tailings and secondary minerals are given in Table 1. Elements with very low concentrations or below the detection limits of the ICP are not presented. All tailings (ZG1–ZG7) had low total sulfur concentrations. Surface samples contained more sulfur than those of the bottom. With the exception of ZG1, sulfur in tailings was mostly in the sulfate form, indicating a highly weathered state along the entire depth of the trenches. Secondary minerals, which probably correspond to either secondary sulfates or to Fe hydroxide sulfates (M1–M4) and Fe oxyhydroxides (M5), had higher total sulfur content.

The Al concentrations were relatively high in the tailings and the secondary minerals, while Ca, Mg, and Mn were generally low in the tailings. The most abundant trace elements were: Ti, Zn, Pb, and As. Other elements present at significant amounts in the studied materials included: Cu, Cr, Co, Ba, Ni, Mo, and Cd. The Zgounder ore was mostly an Ag-Hg amalgam, but the Ag and Hg concentrations were low in the analyzed tailing samples, which means that the cyanide extraction process was complete.

Mineralogical characterization, carried out mainly by XRD, identified silicates and aluminosilicates. The ZG5 sample contained more actinolite than ZG2 and ZG7. It also contained labradorite, orthoclase, wollastonite, and dolomite (Table 1). A hydrated ferric iron sulfate (butlerite) and iron oxide (hematite) were observed in the ZG2 and ZG7 samples. Butlerite generally results from pyrite oxidation. Titanite (also known as sphene) was identified only in the ZG2 tailings. Note that amorphous phases are not detected by XRD.

Mineralogical characterizations completed for the 'unweathered' samples (ZG2, ZG5, and ZG7) using an optical microscope and SEM showed the presence of some sulfides, such as sphalerite (Electronic Supplementary Material Fig. S2a) and galena in the three samples, as well as pyrite in ZG5 and ZG7 (Fig. S2b). In addition, the EDS microanalyses of the pyrite grains indicated the presence of As trace impurities. The arsenopyrite form represented 61.5 % of the pyrite grains in ZG5 (As concentrations within pyrite ranged from 0.45 to 1.73 wt%), while, it represents 33 % of the pyrite grains in ZG7 (containing 0.62–1.5 wt% As). Iron oxides were frequently observed in all samples. As shown in Fig. S2c, iron oxides contain As

Table 1 Physical, chemical and mineralogical characterizations of the studied samples

		Trench T1		Trench T2			Trench T3		Secondary minerals				
		ZG1	ZG2	ZG3	ZG4	ZG5	ZG6	ZG7	M1	M2	M3	M4	M5
Physical characteristics													
G_s		2.84	2.82	2.83	2.83	2.92	2.80	2.80	nd	nd	nd	nd	nd
S_s (m^2 g^{-1})		nd	12.7	nd	nd	8.35	nd	2.94	nd	nd	nd	nd	nd
% <80 (μm)		83.0	35.2	95.0	95.0	40.5	44.6	154	nd	nd	nd	nd	nd
D_{10} (μm)		4.1	3.6	4.1	4.1	3.7	4.0	19.6	nd	nd	nd	nd	nd
D_{50} (μm)		29.8	10.5	24.7	24.7	12.3	19.6	88.6	nd	nd	nd	nd	nd
D_{90} (μm)		126	63.2	149	149	76.3	81.2	187	nd	nd	nd	nd	nd
Chemical characteristics (%)													
Major elements (%)													
Al		8.77	9.24	8.56	9.31	8.96	6.96	4.45	4.05	5.20	6.12	4.09	5.50
Ca		1.47	0.43	1.39	1.02	2.93	0.14	0.07	0.91	0.54	2.86	0.84	1.33
Mg		1.73	1.23	1.74	1.45	2.46	0.76	0.85	0.43	1.20	1.20	1.07	1.13
Mn		0.15	0.06	0.14	0.10	0.27	0.05	0.07	0.09	0.17	0.15	0.15	0.15
Fe		6.59	5.89	6.94	6.09	8.45	4.99	4.77	3.87	4.38	4.23	3.61	13.63
S_{total}		0.41	0.11	0.35	0.26	0.27	0.60	0.23	6.12	3.38	5.62	6.35	1.06
$S_{sulfate}$		0.37	0.15	0.23	0.28	0.20	0.44	0.13	nd	nd	nd	nd	nd
$S_{sulfide}$		0.44	0.05	0.10	0.01	0.06	0.10	0.12	nd	nd	nd	nd	nd
Metals and metalloids (mg kg^{-1})													
Ag		nd	32	nd	nd	16	nd	68	nd	nd	nd	nd	nd
As		520	542	669	751	276	591	560	410	763	534	416	2290
Ba		573	459	493	518	720	332	146	328	285	401	306	373
Cd		<5	<5	<5	<5	<5	<5	<5	<5	72.6	15.8	23.8	64.7
Co		58	33	64	46	133	37.3	36.8	133	188	110	109	150
Cr		112	125	113	117	142	98.2	92.3	67.3	79.1	75.2	70.0	93.6
Cu		278	108	249	216	106	290	237	94.3	294	135	187	54.4
Hg		nd	3.6	nd	nd	5	nd	7.1	nd	nd	nd	nd	nd
Mo		48	50	48	51	73	43	38.3	48.9	65.5	44.5	36.7	367
Ni		23	12	16	11	45	15.7	17.6	18.2	108	11.5	26.8	45.4
Pb		979	826	522	802	390	1204	818	405	609	570	476	381
Ti		8892	5381	9145	6767	10,640	3832	5379	4365	5226	5844	5204	6160
Zn		2511	881	1507	1232	4240	1149	999	2308	23,300	4600	8576	32,120
ABA parameters (kg $CaCO_3$)													
AP		25.03	6.05	10.23	9.04	7.87	16.92	7.95	191.34	106	176	198.5	33.16
NP		4.85	8.38	9.60	6.24	11.06	5.08	4.01	22.91	29.33	76.79	6.74	164
NNP		−8.74	6.89	6.41	5.95	9.29	1.85	0.19	54.07	32.05	116.16	56.3	166.9
NP/AP		0.36	5.63	3.00	21.48	6.24	1.57	1.05	−0.74	−10.79	−1.95	−0.14	−59.01
Minerals (%)	Formulae												
Muscovite	$KAl_2(Si3Al)O_{10}(OH{\cdot}F)_2$		31.2			11.1		27.6					
Albite	$NaAlSi_3O_8$		19.1			15.9		25.5					
Quartz	SiO_2		30.3			7.5		31.4					
Chlorite	$(Fe{\cdot}Mg{\cdot}Al)_6(Si{\cdot}Al)_4O_{10}(OH)_8$		13.6			15.8		11.9					
Actinolite	$(Fe{\cdot}Mg{\cdot}Al)_6(Si{\cdot}Al)_4O_{10}(OH)_8$		1.6			18.8		<1					
Titanite	$CaTiSiO_5$		<1										
Butlerite	$Fe(SO_4)(OH){\cdot}2(H_2O)$		2.9					2.3					
Hematite	Fe_2O_3		<1			<1		<1					
Labradorite	$(Ca{\cdot}Na)(Si{\cdot}Al)_4O_8$					17.9							
Dolomite	$CaMgCO_3$					<1							
Wollastonite	$CaSiO_3$					2.5							
Orthoclase	$KAlSi_3O_8$					9.8							
Total			98.7			99.3		98.7					

ABA acid base accounting (static test), *nd* not determined

(1.42–3.29, 0.45–5.46, and 1.1–1.8 wt% respectively in ZG2, ZG5, and ZG7). Iron oxides within tailings can have a primary but most probably a secondary origin. Indeed, SEM observations showed Fe oxides possibly resulting from the pyrite alteration (Fig. S2b). Also, several Fe oxides contain Zn, Cu, and S, indicating likely secondary trapping of these elements (Fig. S2c). Hemo-ilmenite and ilmenite were identified in the ZG2 and ZG5 tailings, while ilmenite and rutile were observed in the ZG7 sample. Other minerals that were frequently observed by SEM–EDS were similar to those identified by XRD. These include plagioclase (albite, labradorite, bytownite, etc.), amphibole (actinolite and other magnesio-amphibole), chlorite, muscovite, and orthoclase. Apatite was identified in all samples as an accessory mineral. Titanite and barite were observed in the ZG5 tailings.

The mineralogical and chemical analyses (Table 1; Figure S2) show that Al is associated with muscovite, albite, chlorite, labradorite, and orthoclase in the tailings. The Ca is associated principally with plagioclase and amphibole and secondarily with wollastonite, titanite, dolomite, and apatite. The Mg is related to amphibole minerals (actinolite mostly), chlorite, and dolomite. The Fe is related to chlorite, actinolite, ilmenite, oxides (hematite and other unidentified oxides observed by SEM), and sulfides (mostly pyrite) in the tailings samples. The sphalerite and galena can explain the Zn, and Pb concentrations in the tailings. Furthermore, the As is preferentially associated with pyrite and Fe-oxides. No arsenic sulfide was mineralogically identified, although arsenopyrite was described as abundant in the deposit mineralization (Macroux and Wadjinny 2005; Petruk 1975) and was observed in the waste rocks. The Ti is associated with ilmenite, hemo-ilmenite, rutile, and titanite, which was widely observed with the SEM. Sulfide-S is associated mainly with pyrite, sphalerite, and galena. The sulfate-S is related to butlerite, which forms at low pH, which is consistent with its identification at ZG2 and ZG7 and its absence at ZG5 (Murray et al. 2014).

Acid Potential Generation Assessment

Zgounder tailings characterization showed generally low AP and NP values (Table 1). The NP could be underestimated, as it was determined on the basis of carbonate as the only neutralizing minerals (inorganic carbon), while neutralization could have been associated rather with silicates than carbonates (Blowes et al. 1998; Miller et al. 2010; Plante et al. 2011).

Based on the classification of Miller et al. (1991), the NNP values classified the studied wastes as uncertainty. Referring to the NP/AP ratio (Adam et al. 1997), only ZG1 was acid generating. The other tailings were uncertain. Even considering the total sulfur content instead of sulfide-S (Sobek et al. 1978), the NNP remained in the uncertain zone for the tailings samples (except ZG1). Conversely, the NP/AP ratio indicated acid generation for all tailings samples except ZG5. The levels of sulfide-S (and sulfur in general) were very low in these materials, around the limit of uncertainty. ABA interpretation in such cases is difficult. Therefore, kinetic tests were needed to predict the acid generation potential.

Zgounder Tailings Water Leachability

The leaching test results are presented in Fig. 3. The pre-filtration pH of the slurries were acidic (ZG2 and ZG7) to slightly acidic and near neutral (ZG5). After a slight increase at the beginning (between 0 and 2 h), the pH remained stable until the end of the test. SO_4, Ca and Mg were leached mainly during the early hours of the test (Fig. 3). Several trace elements (Zn, As, Mn, Fe, Cu, and Co) were released as soon as the materials were in contact with water, before oxidation could occur. These results indicate that the tailings contain soluble minerals (most probably as secondary phases) that dissolved rapidly, releasing their trace metal and metalloid contents. Even though the mineralogical analyses only identified butlerite, other secondary minerals could be present but not identifiable by XRD because they were amorphous (Hakkou et al. 2008) or below detection limits.

Weathering Cells Results

The geochemical behavior of the tailings is shown in Fig. 4. The graphs correspond to the concentrations released, without normalization (i.e. considering neither the volume nor the mass of samples).

The tailings produced two types of drainages: AMD (ZG2 and ZG7) and CND (ZG5). Indeed, the pH of the leachates were acid for ZG2and ZG7, and near-neutral for ZG5. The pH didn't vary significantly throughout the tests for the three samples. The acidic pH (mainly in ZG2 and ZG7) could be partly due to sulfide oxidation, but the low sulfide levels in the tailings indicate that oxidation alone cannot explain the observed pHs, which are most likely due to dissolution of acidic soluble salts, as shown by the leaching test. In fact, acidity can be explained by hydrolysis of Fe released following oxidation/dissolution (Jambor and Blowes 1998; Skousen et al. 1997). The higher pH in the ZG5 weathering cell tests (also observed in the leaching test) could be explained by the presence of labradorite, bytownite, dolomite, and actinolite (minerals not identified or very low in ZG2 and ZG7). Indeed, calcic plagioclase and amphibole can limit acid production, as these silicates can react rapidly enough to match the rate of acid generation (Edmond Eary and Williamson 2006; Plante et al.

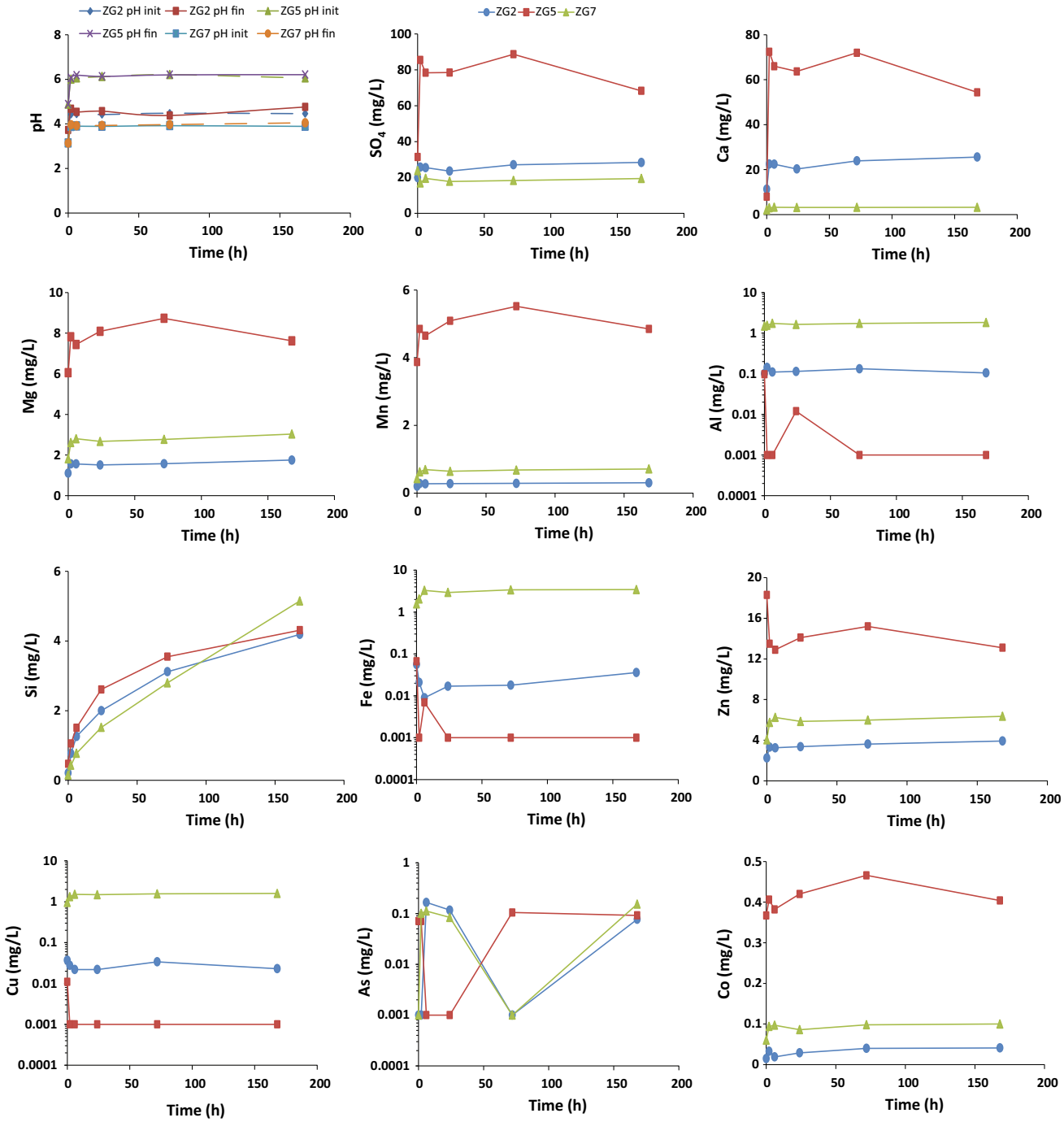

Fig. 3 Water leaching test results (log scale for Al, Cu, Fe, and As)

2011). Dolomite, although present at low concentrations, would also have contributed to alkalinity.

The EC values were higher in the ZG5 leachates than in the ZG2 and ZG7 leachates, indicating more reactivity in the case of ZG5. The Eh values were relatively high, indicating an oxidizing medium, and were comparable for the three samples.

Sulfate concentrations were high at the beginning of each test for the three samples. The SO_4 leached during the first five cycles were higher for ZG5 than for ZG2 and ZG7. From the 45th day on, the trends for SO_4 decreased and stabilized to similar concentrations for all three. The SO_4 in the leachates presumably originated from sulfate dissolution initially, and then from sulfide oxidation later. Ca and Mg showed similar trends to that of SO_4. The released Ca is mainly associated with incongruent dissolution/hydrolysis of plagioclase minerals and actinolite, and from dolomite dissolution. Ca could also come from

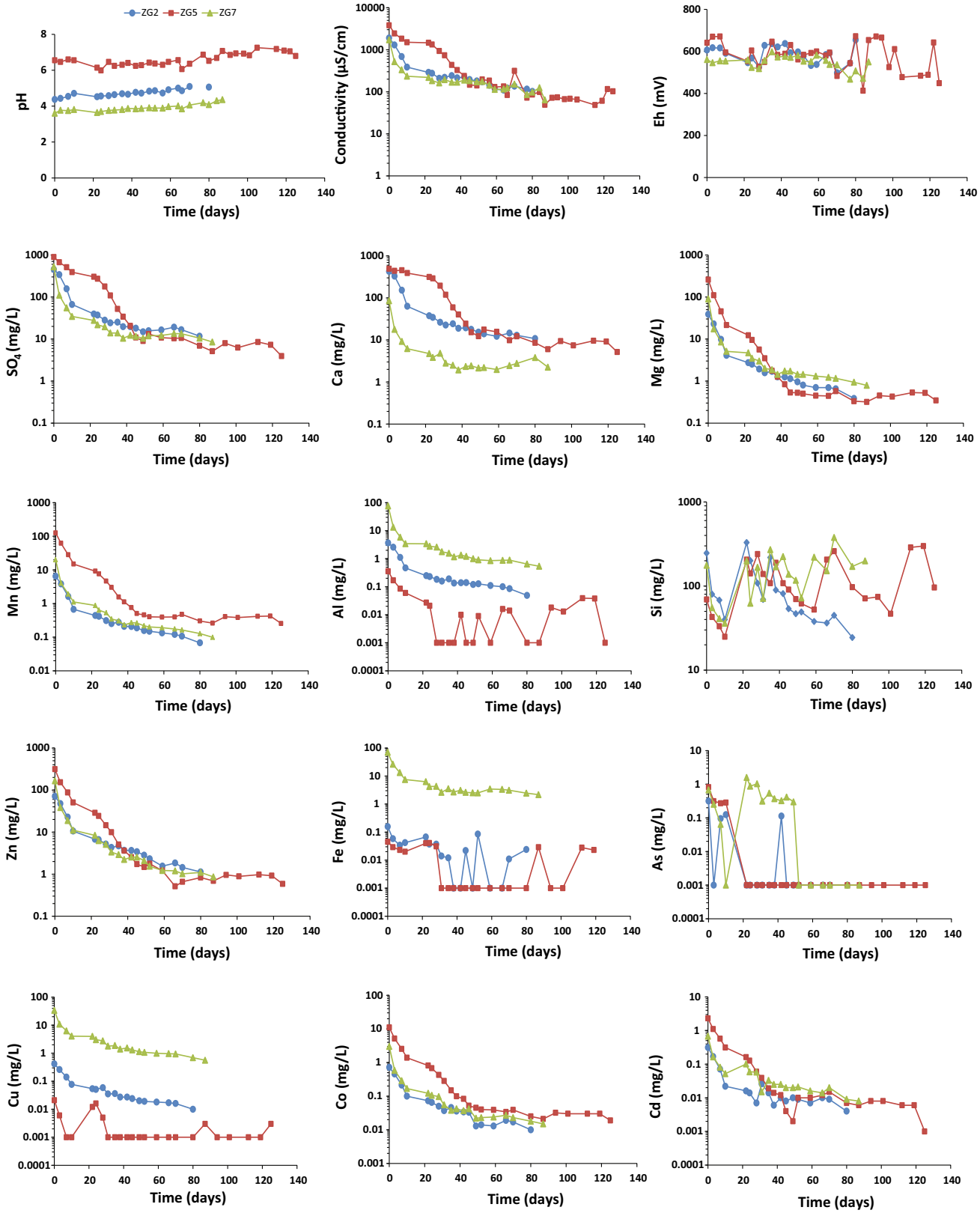

Fig. 4 Leachate quality from weathering cell for the Zgounder tailings samples (log scale for all except pH and Eh)

wollastonite. The Ca concentrations of ZG5 are higher than those in ZG2, which are higher than those of ZG7 (Fig. 4), due most likely to the higher proportion of Ca-rich plagioclases such as bytownite and labradorite, as well as actinolite, in ZG5. Also, dolomite was only identified in ZG5. The ZG2 sample contained more actinolite than ZG7, which explains the greater Ca release in ZG2. The Mg could have come from actinolite and dolomite dissolution, and to a lesser extent, from chlorite alteration. In this case, the larger concentrations of actinolite, dolomite, and chlorite in ZG5 were responsible for the higher Mg concentrations. Moreover, the more acidic pH and less buffering capacity of ZG7 led to greater chlorite reactivity. Indeed chlorite, which has moderate reactivity at pH 5 (Kwong 1993), becomes very reactive at pH <3.

Mn concentrations increased throughout the tests, although no Mn-minerals were identified. The Al was leached at low levels, generally with the highest concentrations observed in the ZG7 tests. The Al levels were initially high for the three tailings, but decreased and tended to stabilize for ZG2 and ZG7, whereas they were variable for ZG5 (Fig. 4). The Al comes mainly from labradorite and chlorite alteration reactions. The albite, muscovite, and orthoclase contribute less because they have slower hydrolysis reactions at pH 5 (Kwong 1993). The acidic pH, favorable to aluminosilicate reactivity, could explain the significant Al concentrations in ZG7. In addition, precipitation of Al as a secondary hydroxide at pH values above 4.5, could have controlled the Al concentration in the ZG5 leachates (Blowes and Ptacek 1994). Significant concentration fluctuations were also observed in the Si released throughout the tests, for all samples. Several phases (actinolite, labradorite, chlorite, albite, muscovite, titanite, and wollastonite) might control Si release, but actinolite most likely explains it.

The As concentrations were low in the weathering test leachates (<1 mg L^{-1}) despite its high concentration in the initial solid phase samples. As is leached following pyrite oxidation and dissolution of Fe oxides as these minerals are most associated with high As contents. Fe in the leachates is related principally to pyrite oxidation and dissolution of Fe oxyhydroxides, and secondarily to chlorite and actinolite alteration. However, its concentrations are significant only for ZG7. This is explained by Fe precipitation at relatively low pH (pH >4) (Gunsinger et al. 2006; Holmström et al. 1999).

The most significant Cu release was observed for ZG7. Cu is an amphoteric metal with low mobility at neutral pH, and it remains adsorbed even at low pH (pH 4) (Gunsinger et al. 2006). Cu desorption requires pH values below 3 (Galán et al. 2003; Jurjovec et al. 2002); thus, its release from the tailings is likely related to Fe oxides, which contain significant Cu, based on SEM–EDS analysis. Cu could also have been come from chalcopyrite oxidation even if the latter was not clearly identified in the tailings. Chalcopyrite was observed in the waste rocks samples and has been widely described in the ore deposit mineralization (Macroux and Wadjinny 2005; Petruk 1975). Release of Zn was higher than Fe and Cu for the three samples. Zn originates from sphalerite oxidation and dissolution of Fe oxides, which contain Zn (0.4–4.4 %). Cd was mainly present during the first leaching cycle, with concentrations >1 mg L^{-1}. The Cd leaching trends were similar to those of Zn. The Cd might originate from sphalerite dissolution as well; Cd was identified in sphalerite by SEM analyses (Fig. S2) and was also described in the deposit mineralization (Macroux and Wadjinny 2005). The Co was relatively significant for ZG5 during the two first weeks of leaching.

The SO_4, Ca, and Mg in the leachates were normalized to the total sample mass and the volume recovered in each leaching test, then summed (mg kg^{-1}). The slope of the linear regression for the stabilized portion of these cumulative normalized loadings over time (Fig. 5) provides the elemental release rates (mg kg^{-1} day^{-1}). The cumulative SO_4, Ca, and Mg levels of ZG5 were significantly greater than those of ZG2 and ZG7 (Fig. 5a, c, e). The SO_4 release rate was much greater for ZG5 (1.2 mg kg^{-1} day^{-1}) than for ZG2 (0.4 mg kg^{-1} day^{-1}) and ZG7 (0.5 mg kg^{-1} day^{-1}). The relative difference was even more pronounced for Mg release rates (ZG5: 25.8 mg kg^{-1} day^{-1}, ZG2: 6.7 mg kg^{-1} day^{-1}, ZG7 3.6 mg kg^{-1} day^{-1}). However, Ca release rates were higher in ZG7 than ZG2 and ZG5.

The dissolved SO_4, Ca, and Mg stabilized, and reaction rates decreased, from the fifth cycle for ZG5 and the second cycle for ZG2 and ZG7, indicating depletion of the more reactive solid phases (Lappako 2000) and precipitation of secondary minerals (Aubertin et al. 2002). Passivation following the precipitation of secondary minerals could also be a contributing factor (Belzile et al. 2004; Cruz et al. 2001).

The cumulative masses of sulfate measured in the leachates were plotted versus the cumulative amounts of Ca + Mg (oxidation–neutralisation curve; Benzaazoua et al. 2004). Sulfate represents the main oxidation product whereas Ca + Mg represents the principal carbonate minerals (although low) and silicate dissolution products (Fig. 5b, d, f). The curves were approximately linear in all of the weathering cell tests, which indicate that the neutralizing minerals react specifically to the acid produced by the three studied tailings, similar to observations by Benzaazoua et al. (2004) for different materials.

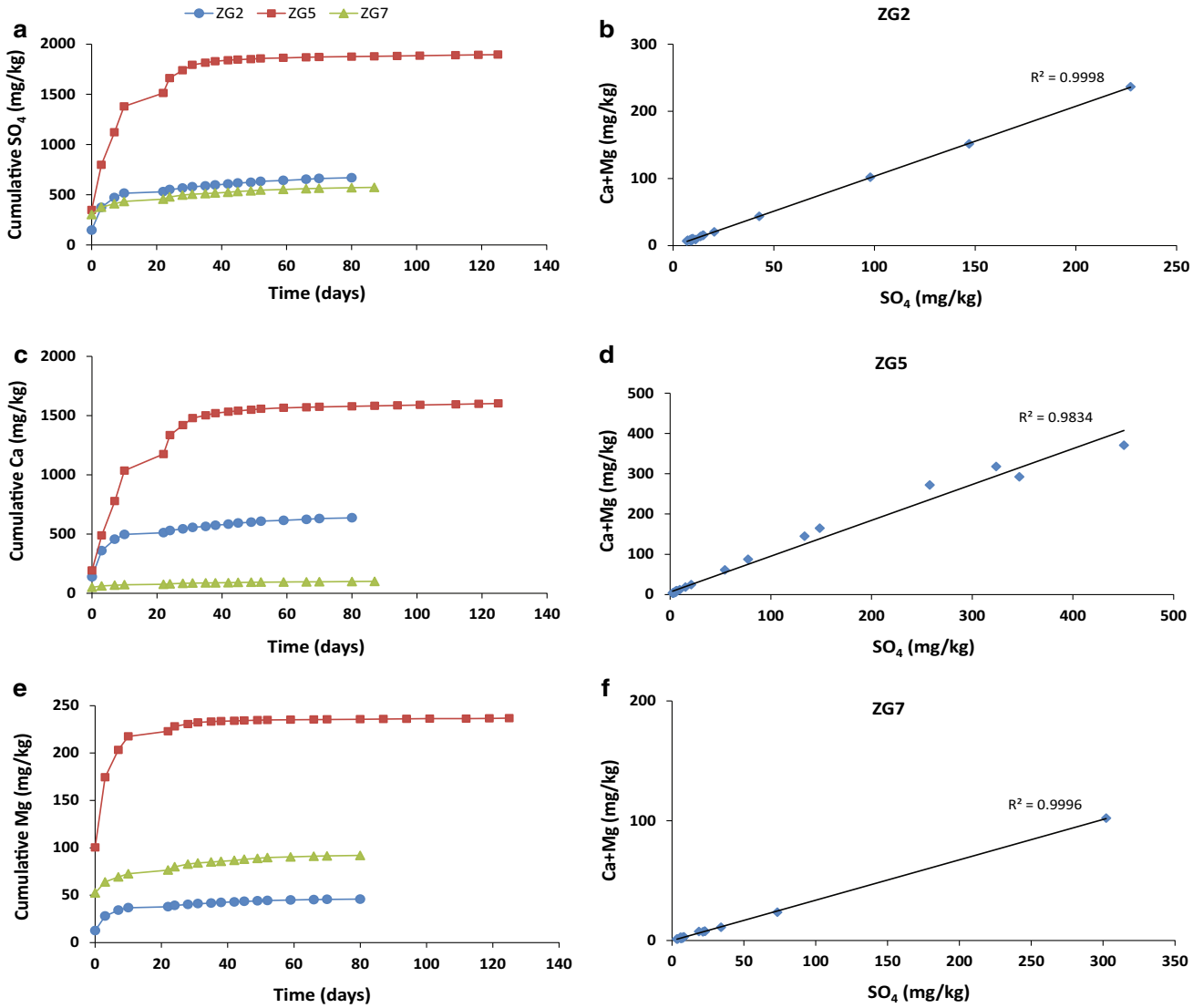

Fig. 5 Evolution of cumulative masses of SO_4 (**a**), Ca (**c**), and Mg (**e**) collected throughout the weathering test and oxidation–neutralization curve (cumulative Ca + Mg loads vs cumulative SO_4) for ZG2 (**b**), ZG5 (**d**) and (**f**) ZG7

Discussion

Factors Controlling the Zgounder Mine Drainage

The tailings produce both AMD (ZG2 and ZG7) and CND (ZG5). This difference in acid generation potential for the different north tailings pond samples could be due to changes in the geology, type of exploitation, or beneficiation over time. ZG5 most probably corresponds to an ore zone richer in neutralizing minerals.

In most cases of AMD, sulfide oxidation (mainly Fe-sulfide) is the principal phenomenon responsible for acidity generation and metal release. At Zgounder, the tailings sulfide content was low, yet the leachate obtained (in the leaching and weathering cells tests) for ZG2 and ZG7 was acidic. Although the relatively low amounts of sulfides might have contributed acidity, dissolution of secondary metal-sulfate salts and hydrolysis of Fe hydroxides seem to be the main reasons for the acidity produced by these samples, as reported by Harris et al. (2003) and Jambor and Blowes (1998). The lack of neutralizing minerals in the tailings increased the acidity. The greater proportion of suitable neutralizing minerals at ZG5 provided more buffering capacity, which neutralized the acidity produced by the same weathering reactions.

Some of the elements released by oxidation, neutralization, and dissolution precipitate in the saturated pore spaces or on the surface of solid particles, as secondary minerals (Haffert et al. 2010; Harris et al. 2003; Mahoney et al. 2005; Murray et al. 2014). Secondary salts observed on the surface

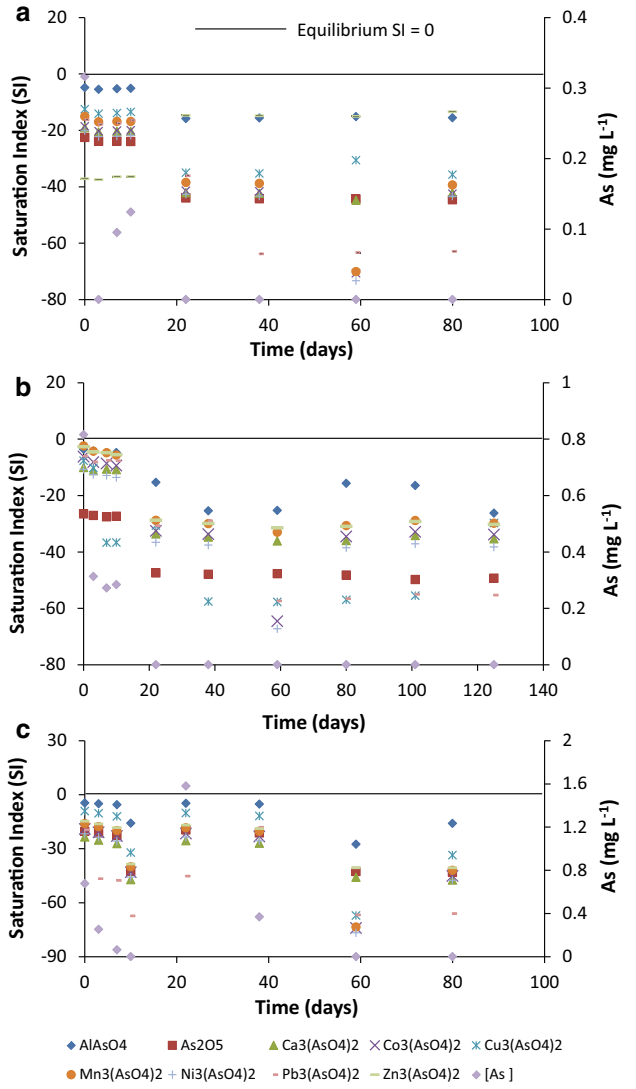

Fig. 6 Evolution of saturation indices of the As secondary phases during weathering cell tests for ZG2 (**a**), ZG5 (**b**) and ZG7 (**c**)

of the tailings ponds (samples M1–M5), as well as those formed in the tailings and dissolved during testing, demonstrate these reactions. In an arid climate, like the climate of the mine site, evaporation increases salt formation during the summer (Hakkou et al. 2008; Hammarstrom et al. 2005). However, these efflorescent minerals are dissolved with the first flush of rains in the wet season, leaching their solutes to be transported downstream to the Zgounder River. Indeed, rain water and seepage collected on the surface of the north tailings pond had a relatively low pH (5.4–6.4) and significant contamination, which exceed (for some) those obtained experimentally (SO_4: 1016–7785 mg L^{-1}, Fe: 15–47.5 mg L^{-1}, and Zn: 6–12.8 mg L^{-1}).

Sorption mechanisms also contribute to drainage quality. Some elements (As in particular) present at high proportions in the tailings were not detected or were present at very low concentrations in the leachates. This implies that the As is being sequestered in the solid phase (solid solution/co-precipitation) rather than being leached during periods of wetting and runoff (Fukushi et al. 2003). Precipitation of As is improbable, given the leachate pH and thermodynamic equilibrium calculations performed with Visual MINTEQ. Indeed, all As potential secondary phases were undersaturated (negative saturation indices) for the three weathering tests (Fig. 6). Sorption tests discussed below verified the As sorption hypothesis.

As Sorption in Tailings Samples

The kinetic and static sorption test results are presented in Fig. 7. The sorption kinetics show rapid sorption of As for all tests (Fig. 7a, b). After only 2 h, more than 99 % of the As was taken up by the ZG2 and ZG7 tailings and over 88 % in the case of ZG5 (Fig. 7b). The rapid As uptake during the first minutes of the experiments indicated a significant sorption capacity and enabled us to estimate that a 24 h (1440 min) test would be long enough to achieve equilibrium conditions. Batch sorption tests were used to evaluate the sorption capacities for different As concentrations and pHs. The sorption capacities at equilibrium (q_e) for 10 mg L^{-1} of As at pH 4, 5, 6, and 7 are shown in Fig. 7c–g. Figure 7c shows the amount of As sorbed. The sorption capacities were normalized for mass (mg kg^{-1}, Fig. 7e) and Ss area (mg m^{-2}, Fig. 7g). The Ss areas were considered to account for different grain-size distributions. The sorption capacities normalized to Ss areas were obtained by dividing the sorption capacities per the masses (mg kg^{-1}) using the respective Ss areas measured in the samples (m^2 kg^{-1}).

The As sorption was very similar for all of the materials at all pHs tested with more than 90 % sorption. The absence of preferential sorption as a function of pH is due to the acidic to neutral pH at which the tests were conducted. In these conditions, As(V) sorption (mainly by Fe oxides) is maximized and decreases only at alkaline pH (>8, 9, or 11 depending on the sorbents) (Carrillo and Drever 1998; Giménez et al. 2007; Mamindy-Pajany et al. 2011). The ranges were greater for ZG2 than for ZG5 and ZG7. On a Ss area basis, the sorption capacity of ZG7 greatly exceeded that of ZG2 and ZG5. Given that:

(1) Sorption capacities were high at all tested pH values and did not show significant differences,
(2) No differences were noted for preliminary tests conducted at 'optimum' pH (pH 7 for ZG2 and at pH 4 for ZG5 and ZG7), and
(3) The differences between the three samples was minimized at pH 6,

a pH of 6 was selected to study the effect of As concentration (0.1, 1, 10, and 50 mg L^{-1} As) on sorption behavior

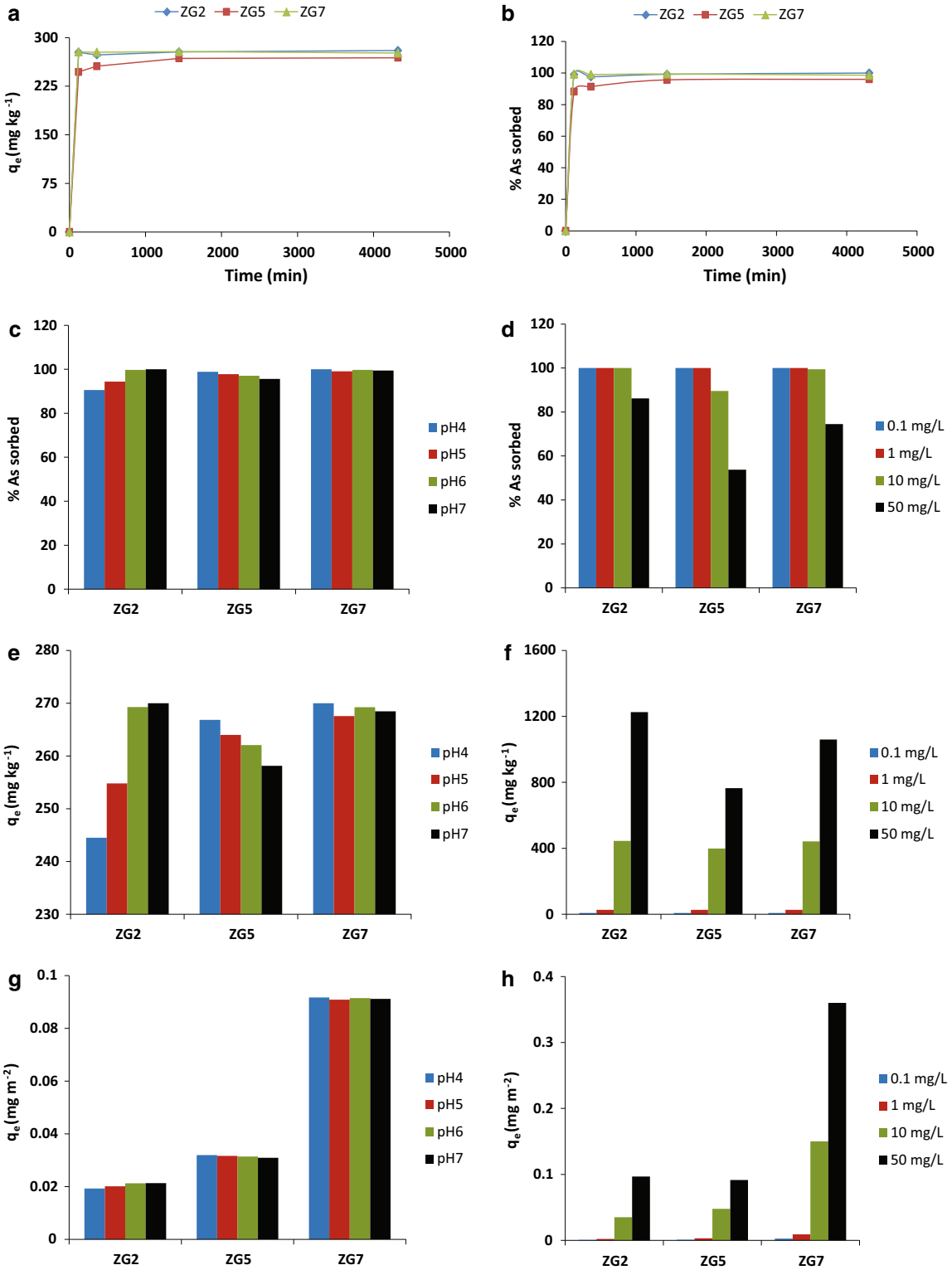

Fig. 7 Arsenic sorption kinetics in 0.05 M $NaNO_3$, pH 6 and 10 mg L^{-1} As (**a**, **b**), % As sorbed (**c**) and As sorption capacities (q_e): at pH 4, 5, 6 and 7 for 1:25 mg L^{-1} As (per mass, **e** and per surface area, **g**) and at pH 6 for 0.1, 1, 10 and 50 mg L^{-1} (**d**, **f**, **h**)

(Fig. 7d–h). The high As sorption capacities of the three tailings were confirmed. The As was 90–100 % sorbed at 0.1, 1, and 10 mg L^{-1} As (Fig. 7d). At a concentration of 50 mg L^{-1}, As uptake was greater in ZG2 and ZG7, and less for ZG5. The decrease in the amounts sorbed at high As concentrations can be explained by partial saturation of

the surface sites of sorbent minerals (Carrillo and Drever 1998; Mamindy-Pajany et al. 2009). ZG7 showed the highest As sorption capacity on a Ss area basis (Fig. 7h). However, ZG7 is coarser-grained, with a lower Ss area than ZG2 and ZG5. Usually, As sorption is more important when the material is finer (Carrillo and Drever 1998). This result could be explained by the mineralogical nature of the ZG7 sample, which presumably has (or has in higher concentrations) mineralogical phases with high As uptake potentials that can compensate for its lower Ss area. This mineralogical phase could be rutile, which was only identified in ZG7 by SEM analyses and is known for its significant As sorption capacity (Dutta et al. 2004; Yan et al. 2014). The mineralogical composition could also explain the lower sorption rate noted in ZG5, compared to ZG2 and ZG7.

Sequential Extractions

Sequential extractions were performed on ZG2, ZG5, and ZG7 tailings to assess the nature of the sorption sites (Electronic supplementary Material Fig. S3). The three tailings samples show a similar As speciation. More than 99 % of the extracted As is bound in the reducible phases (Fig. S3b). The acid soluble (0.12–0.76 %) and soluble/exchangeable (0.05–0.17 %) fractions is insignificant (Fig. S3b). Thus, the results show that the principal sorption sites were associated with the reducible species; other As uptake sources are negligible. These reducible species in the solid phase are generally considered to be Fe and Mn oxides and oxyhydroxides. It is well known that As in mine tailings is strongly associated with Fe-oxyhydroxides (e.g. García-Sánchez et al. 2010; Kim et al. 2012; Palumbo-Roe et al. 2007). Several Fe oxides were identified by XRD/SEM for the three samples, including hematite, which has a large affinity for As sorption (Giménez et al. 2007; Mamindy-Pajany et al. 2011). Fe-oxides seem to be most likely responsible for the attenuation of As in the Zgounder drainage (Asta et al. 2009).

Sequential extractions performed after the weathering cell tests ended showed no As distribution changes compared to initial samples. Extracted As still came from the reducible phases (Fig. S3c, d). This indicates that the As released was again sorbed preferentially by Fe-oxyhydroxides (Mamindy-Pajany et al. 2011).

Conclusions

Zgounder tailings generate AMD or CND depending on their location. The AMD is mainly produced by dissolution of metal sulfate salts and Fe hydrolysis rather than by sulfide oxidation. The abundance of neutralizing minerals varies spatially across the site; hence the CND noted for some areas of the tailings pond. Neutralization is provided primarily by silicate minerals, mainly Ca-plagioclases (labradorite and bytownite) and amphibole (actinolite). Precipitation and dissolution of acidic salts play important roles in the storage and transport of acidity and trace metals and metalloids, and effectively control the geochemistry of the mine water and the chemistry downstream of the mine.

Sorption has been revealed as a major phenomenon controlling As in the leachate from the tailings. Given the oxidizing conditions, As primarily occurs as the arsenate species. The tested materials show high As sorption capacities that are not pH-dependent at the pH range considered. The minerals comprising the sorbents appear to be responsible for As uptake by the Zgounder tailings. At high As concentrations, the sorption capacities of the tailings can begin to be saturated. Most sorption sites are associated with reducible mineral fractions, probably Fe-oxyhydroxides. Thus, reducible phases naturally attenuate As in the Zgounder tailings drainage.

The results from this study provides information on the geochemical behavior of the Zgounder wastes and on the phenomena controlling the chemistry of drainage waters, with a focus on the As sorption phenomena. Additional studies are needed for better identification of the mineralogical phases (salts and secondary minerals) involved in contaminant sequestration and leaching. Further studies are also necessary to better understand the mechanisms involved in As sorption. These investigations should:

- Identify which reductible phases sorb As, and the nature of As retention, in order to assess the long-term stability of the As-solid phase interactions.
- Assess the As sorption under reducing conditions that might occur in the field (e.g. bottom of the tailings pond).
- Evaluate the effect of competition of other anions such as sulfate on the tailings sorption capacity of As. PO_4 can also compete with As for sorption sites; however this competition is unlikely in the present study given that its only known mineral phase at this site has very low solubility (apatite).
- Assess the As desorption rate after saturation of the tailings or changes in the geochemistry in the tailings.

Acknowledgments Financial support for this study was provided through the International Research Chairs Initiative, a program funded by the International Development Research Centre (IDRC) and by the Canada Research Chairs program (Canada).

References

Adam K, Courtis A, Gazea B, Kontopoulos A (1997) Evaluation of static tests used to predict the potential for acid drainage generation at sulphide mine sites. Trans Inst Min Metal Sect A 106:A1–A8

Akcil A, Koldas S (2006) Acid mine drainage (AMD): causes, treatment and case studies. J Clean Prod 14:1139–1145

Appelo CAJ, Postma D (2005) Geochemistry, groundwater and pollution, 2nd edn. Balkema, London

Asta MP, Cama J, Martínez M, Giménez J (2009) Arsenic removal by goethite and jarosite in acidic conditions and its environmental implications. J Hazard Mater 171:965–972

Aubertin M, Bussière B, Berbier LR (2002) Environnement et gestion des rejets miniers. CD-ROM, Presses internationales de Polytechnique, Paris

Bagherifam S, Lakzian A, Fotovat A, Khorasani R, Komarneni S (2014) In situ stabilization of As and Sb with naturally occurring Mn, Al and Fe oxides in a calcareous soil: bioaccessibility, bioavailability and speciation studies. J Hazard Mater 273:247–252

Beauchemin S, Kwong YTJ (2006) Impact of redox conditions on arsenic mobilization from tailings in a wetland with neutral drainage. Environ Sci Technol 40:6297–6303

Belzile N, Chen YW, Cai MF, Li Y (2004) A review on pyrrhotite oxydation. J Geochem Explor 84:65–76

Benzaazoua M, Bussière B, Dagenais AM, Archambault M (2004) Kinetic tests comparison and interpretation for the prediction of the Joutel tailings acid generation potentiel. Environ Geol 46:1086–1101

Blowes DW, Ptacek CJ (1994) Acid-neutralization mechanisms in inactive mine tailing. In: Jambor J, Blowes D (eds) Schort course handbook on environmental geochemistry of sulfide mine-wastes. Mineralogical Society of Canada, Ottawa, pp 271–292

Blowes DW, Jambor JL, Hanton-Fong ChJ (1998) Geochemical, mineralogical and microbiological characterization of a sulphide-bearing carbonate-rich gold-mine tailings impoundment, Joutel, Québec. Appl Geochem 13(6):687–705

Brunauer S, Emmett PH, Teller E (1938) Adsorption of gases in multimolecular layers. J Am Chem Soc 6:309–319. https://zumbuhllab.unibas.ch/pdf/refs/BET_JACS_1938.pdf

Carrillo A, Drever JI (1998) Adsorption of arsenic by natural aquifer material in the San Antonio-El Triunfo mining area, Baja California, Mexico. Environ Geol 35(4):251–257

Cheng H, Hu Y, Luo J, Xu B, Zhao J (2009) Geochemical processes controlling fate and transport of arsenic in acid mine drainage (AMD) and natural systems. J Hazard Mater 165:13–26

Cruz R, Mendez BA, Monroy M, Gonzalez I (2001) Cyclic voltammetry applied to evaluate reactivity in sulfide mining residues. Appl Geochem 16:1631–1640

Dold B (2003) Speciation of the most soluble phases in a sequential extraction procedure adapted for geochemical studies of copper sulphide mine waste. J Geochem Explor 80:55–68

Drahota P, Filippi M, Ettler V, Rohovec J, Mihaljevič M, Šebek O (2012) Natural attenuation of arsenic in soils near a highly contaminated historical mine waste dump. Sci Total Environ 414:546–555

Dutta PK, Ray AK, Sharma VK, Millero FJ (2004) Adsorption of arsenate and arsenite on titanium dioxide suspensions. J Colloid Interface Sci 278:270–275

Edmond Eary L, Williamson MA (2006) Simulations of the neutralizing capacity of silicate rocks in acid mine drainage environments. In: Barnhisel RI (eds) Proceedings of the 7th international conference on acid rock drainage (ICARD). American Society of Mining and Reclamation (ASMR), Lexington, KY, USA, pp 564–577. http://www.asmr.us/Publications/Conference%20Proceedings/2006/0564-Eary-Co.pdf

Expertise Center in Environmental Analysis of Quebec (2012) Protocole de lixiviation pour les espèces inorganiques, MA. 100 – Lix.com.1.1, Rév. 1, Ministère du Développement durable, de l'Environnement, de la Faune et des Parcs du Québec, Canada

Foli G, Gawu SKY, Manu J, Nude PM (2013) Arsenic sorption characteristics in decommissioned tailings dam environment at the Obuasi Mine, Ghana. Res J Environ Earth Sci 5(10):599–610

Frostad SR, Price WA, Bent H (2003) Operational NP determination—accounting for iron manganese carbonates and developing a site-specific fizz rating. In: Spiers G, Beckett P, Conroy H (eds) Mining and the environment, Sudbury. Laurentian University, Sudbury, pp 231–237

Fukushi K, Sasaki M, Sato T, Yanase N, Amano H, Ikeda H (2003) A natural attenuation of arsenic in drainage from an abandoned arsenic mine dump. Appl Geochem 18:1267–1278

Galán E, Gómez-Ariza JL, González I, Fernández-Caliani JC, Morales E, Giráldez I (2003) Heavy metal partitioning in river sediments severely polluted by acid mine drainage in the Iberian Pyrite Belt. Appl Geochem 18:409–421

García-Sánchez A, Alonso-Rojo P, Santos-Francés F (2010) Distribution and mobility of arsenic in soils of a mining area (western Spain). Sci Total Environ 408:4194–4201

Giménez J, Martínez M, de Pablo J, Rovira M, Duro L (2007) Arsenic sorption onto natural hematite, magnetite, and goethite. J Hazard Mater 141:575–580

Gunsinger MR, Ptacek CJ, Blowes DW, Jambor JL, Moncur MC (2006) Mechanisms controlling acid neutralization and metal mobility within a Ni-rich tailing impoundment. Appl Geochem 21:1301–1321

Haffert L, Craw D, Pope J (2010) Climatic and compositional controls on secondary arsenic mineral formation in high-arsenic mine wastes, South Island, New Zealand. NZ J Geol Geophys 53:91–101

Hakkou R, Benzaazoua M, Bussière B (2008) Acid mine drainage at the abandoned kettara mine (Morocco): 1. Environmental characterization. Mine Water Environ 27:145–159

Hammarstrom JM, Seal RR II, Meier AL, Kornfeld JM (2005) Secondary sulfate minerals associated with acid drainage in the eastern US: recycling of metals and acidity in surficial environments. Chem Geol 215:407–431

Harris DL, Lottermoser BG, Duchesne J (2003) Ephemeral acid mine drainage at the Montalbion silver mine, north Queensland. Aust J Earth Sci 50:797–809

Holmström H, Jungberg J, Öhlander B (1999) Role of carbonates in mitigation of metal release from mining waste. Evidence from humidity cells tests. Environ Geol 37(4):267–280

Jambor JL, Blowes DW (1998) Theory and applications of mineralogy in environmental studies of sulfide bearing mine wastes. In: Cabri LJ, Vaughan DJ (Eds) Modern approaches to ore and environmental mineralogy, vol 27. Mineralogical Association of Canada Short Course Series, Canada, pp 367–401

Jurjovec J, Ptacek CJ, Blowes D (2002) Acid neutralization mechanisms and metal release in mine tailings: a laboratory column experiment. Geochim Cosmochim Acta 66(9):1511–1523

Kim KR, Lee BT, Kim KW (2012) Arsenic stabilization in mine tailings using nano sized magnetite and zero valent iron with the enhancement of mobility by surface coating. J Geochem Explor 113:124–129

Kwong YTJ (1993) Prediction and prevention of acid rock drainage from a geological and mineralogical perspective. MEND report 1.32.1. CANMET, Ottawa

Lappako K (2000) Kinetic tests. Short course on mine waste characterization and drainage quality prediction. ICARD, Canada, pp 44–59

Lawrence RW, Wang Y (1996) Determination of neutralizing potential for acid rock drainage prediction. MEND/NEDEM report 1.16.3. Canadian Centre for Mineral and Energy Technology, Ottawa

Lawrence RW, Poling GW, Marchant PB (1989) Investigation of predictive techniques for acid mine drainage. MEND/NEDEM

report 1.16.1a. Canadian Centre for Mineral and Energy Technology, Ottawa

Lei L, Song C, Xie X, Li Y, Wang F (2010) Acid mine drainage and heavy metal contamination in groundwater of metal sulfide mine at arid territory (BS mine, Western Australia). Trans Nonferr Metal Soc China 20:1488–1493

Limousin G, Gaudet JP, Charlet L, Szenknect S, Barthes V, Krimissa M (2007) Sorption isotherms: a review on physical bases, modeling and measurement. Appl Geochem 22:249–275

Lizama KA, Fletcher TD, Sun G (2011) Removal processes for arsenic in constructed wetlands. Chemosphere 84:1032–1043

Macroux E, Wadjinny A (2005) The Ag–Hg Zgounder ore deposit (Jebel Siroua, Anti-Atlas, Morocco): a Neoproterozoic epithermal mineralization of the Imiter type. CR Geosci 337(16):1439–1446

Mahoney J, Langmuir D, Gosselin N, Rowson J (2005) Arsenic readily released to pore waters from buried mill tailings. Appl Geochem 20:947–959

Mamindy-Pajany Y, Hurel C, Marmier N, Roméo M (2009) Arsenic adsorption onto hematite and goethite. CR Chim 12:876–881

Mamindy-Pajany Y, Hurel C, Marmier N, Roméo M (2011) Arsenic(V) adsorption from aqueous solution onto goethite, hematite, magnetite and zero-valent iron: effects of pH, concentration and reversibility. Desalination 281:93–99

Merkus HG (2009) Particle size measurements fundamentals, practice, quality. Particle technology series, vol 17, Springer, Berlin. doi:10.1007/978-1-4020-9016-5_6

Miller SD, Jeffery JJ, Wong JWC (1991) Use and misuse of the acid base account for "AMD" prediction. In: Proceedings of the 2nd international conference on acid rock drainage (ICARD), Montréal, Canada, vol 3, pp 489–506

Miller SD, Stewart WS, Rusdinar Y, Schumann RE, Ciccarelli JM (2010) Methods for estimation of long-term non-carbonate neutralization of acid rock drainage. Sci Total Environ 408:2129–2135

Murray J, Kirschbaum A, Dold B, Guimaraes EM, Pannunzio E (2014) Jarosite versus soluble iron-sulfate formation and their role in acid mine drainage formation at the Pan de Azúcar mine tailings (Zn–Pb–Ag), NW Argentina. Minerals 4:477–502

Neculita CM, Zagury GJ, Bussière B (2008) Effectiveness of sulfate-reducing passive bioreactors for treating highly contaminated acid mine drainage: II. Metal removal mechanisms and potential mobility. Appl Geochem 23:3545–3560

Niyogi DK, Lewis WM Jr, McKnight DM (2002) Effects of stress from mine drainage on diversity, biomass, and function of primary producers in Mountain streams. Ecosystems 5:554–567

Palumbo-Roe B, Klinck B, Cave M (2007) Arsenic speciation and mobility in mine wastes from a copper–arsenic mine in Devon, UK: an SEM, XAS, sequential chemical extraction study. Trace Metals Contam Environ 9:431–460

Petruk W (1975) Mineralogy and geology of the Zgounder silver deposit in Morocco. Can Mineral 13:43–54

Plante B, Benzaazoua M, Bussière B, Biesinger MC, Pratt AR (2010) Study of Ni sorption onto Tio mine waste rock surfaces. Appl Geochem 25:1830–1844

Plante B, Benzaazoua M, Bussière B (2011) Predicting geochemical behavior of waste rock with low acid generating potential using laboratory kinetic tests. Mine Water Environ 30:2–21

Potts PJ (1987) A Handbook of silicate rock analysis. Blakie, London

Pöykiö R, Perämäki P, Välimäki I, Kuokkanen T (2002) Estimation of environmental mobility of heavy metals using a sequential leaching of particulate material emitted from an opencast chrome mine complex. Anal Bioanal Chem 373:190–194

Rietveld HM (1993) The Rietveld method. Oxford University Press, London

Skousen J, Renton J, Brown H, Evans P, Leavitt B, Brady K, Cohen L, Ziemkiewicz P (1997) Neutralization potential of overburden samples containing siderite. J Environ Qual 26:673–681

Smedley PL, Kinniburgh DG (2002) A review of the source, behaviour and distribution of arsenic in natural waters. Appl Geochem 17:517–568

Sobek AA, Schuller WA, Freeman JR, Smith RM (1978) Field and laboratory methods applicable to overburdens and mine soils. EPA-600/2-78-054. Washington, DC, pp 47–50

SRK (Steffen Robertson and Kristen) (1989) Acid rock drainage technical guide. BCAMD task force, vol 1. BiTech, Richmond

Tessier A, Campbell PGC, Bisson M (1978) Sequential extraction procedure for the speciation of particulate trace metals. Anal Chem 51(7):844–851

Villeneuve M, Bussière B, Benzaazoua M, Aubertin M, Monroy M (2004) The influence of kinetic test type on the geochemical response of low acid generating potential tailings. In: Proceedings of the tailings and minewaste '03, Sweets and Zeitlinger, Vail, CO, USA, pp 269–279

Yan L, Hu S, Duan J, Jing C (2014) Insights from arsenate adsorption on rutile (110): grazing-incidence X-ray absorption fine structure spectroscopy and DFT+ U study. J Phys Chem 118(26):4759–4765